

# Observation of simultaneous Stokes and anti-Stokes emission in a silicon Raman laser

Ozdal Boyraz, Dimitri Dimitropoulos, and Bahram Jalali<sup>a)</sup>

*Optoelectronic Circuits and Systems Laboratory*

*University of California, Los Angeles*

*Los Angeles, CA 90095-1594*

a) [jalali@ucla.edu](mailto:jalali@ucla.edu)

**Abstract:** We demonstrate a silicon Raman laser and report observation of simultaneous lasing at 1675 nm and parametric Raman emission at 1540 nm. The laser is pumped with 1540 nm pulses and has a threshold at 9 W peak pulse power.

**Keywords:** Waveguides, semiconductor lasers, silicon photonics, Raman

**Classification:** Photonic devices, circuits and systems

## References

- [1] L. Pavesi and D. J. Lockwood, *Silicon Photonics*, Springer-Verlag, New York, 2004.
- [2] G. T. Reed and A. P. Knights, *Silicon Photonics: An Introduction*, John Wiley, West Sussex, 2004.
- [3] L. Pavesi, L. D. Negro, G. Mazzoleni, G. Franzo, and S. Priolo, "Optical gain in silicon nanocrystals," *Nature*, vol. 408, pp. 440–444, 2000.
- [4] J. Ruan, P. M. Fauchet, L. D. Negro, M. Cazzanelli, and L. Pavesi, "Stimulated emission in nanocrystalline silicon superlattices," *Appl. Phys. Lett.*, vol. 83, pp. 5479–5481, 2003.
- [5] S. Saini et al., "High index contrast silicon oxynitride materials platform for Er-doped microphotonic amplifiers," *Proceedings of MRS Spring Meeting*, San Francisco, CA, 2004.
- [6] A. Polman and F. C. J. M. V. Veggel, "Broadband sensitizers for erbium-doped planar optical amplifiers: review," *J. Opt. Soc. Am. B*, vol. 21, pp. 871–892, 2004.
- [7] J. Lee, J. Shin, and N. Park, "Optical gain in Si-nanocrystal sensitized, Er-doped silica waveguide using top-pumping 470 nm LED," *Proceedings of Optical fiber communication conference*, Los Angeles, CA, 2004.
- [8] A. Liu, R. Jones, L. Liao, D. Samara-Rubio, D. Rubin, O. Cohen, R. Nicolaescu, and M. Paniccia, "A high-speed silicon optical modulator based on a metal-oxide-semiconductor capacitor," *Nature*, vol. 427, pp. 615–618, 2004.
- [9] C. A. Barrios, V. R. Almeida, R. Panepucci, and M. Lipson, "Electro-optic modulation of silicon-on-insulator submicrometer size waveguide Devices," *J. Lightwave Technol.*, vol. 21, pp. 2332–2339, 2003.

- [10] J. Oh, S. K. Banerjee, and J. C. Campbell, “Metal-germanium-metal photodetectors on heteroepitaxial Ge-on-Si with amorphous Ge Schottky barrier enhancement layers,” *IEEE Photon. Technol. Lett.*, vol. 16, pp. 581–583, 2004.
- [11] R. Claps, D. Dimitropoulos, Y. Han, and B. Jalali, “Observation of Raman emission in silicon waveguides at 1.54  $\mu\text{m}$ ,” *Optics Express*, vol. 10, no. 22, pp. 1305–1313, Nov. 2002.
- [12] R. Claps, D. Dimitropoulos, V. Raghunathan, Y. Han, and B. Jalali, “Observation of stimulated Raman amplification in silicon waveguides,” *Optics Express*, vol. 11, no. 11, pp. 1731–1739, July 2003.
- [13] R. Claps, V. Raghunathan, D. Dimitropoulos, and B. Jalali, “Anti-Stokes Raman conversion in Silicon waveguides,” *Optics Express*, vol. 11, no. 22, pp. 2862–2872, Nov. 2003.
- [14] K. Suto, T. Kimura, T. Saito, and J. Nishizawa, “Raman amplification in GaP-AlxGa1-xP waveguides for light frequency discrimination,” *IEE Proc.-Optoelectron.*, vol. 145, pp. 105–108, 1998.
- [15] J. I. Dadap, R. L. Espinola, R. M. Osgood, Jr., S. J. McNab, and Y. A. Vlasov, “Spontaneous Raman scattering in a silicon wire waveguide,” *Proceedings of IPR 2004*, San Francisco, CA, USA, paper IWA4, June 2004.
- [16] A. Liu, H. Rong, M. Paniccia, O. Cohen, and D. Hak, “Net optical gain in a low loss silicon-on-insulator waveguide by stimulated Raman scattering,” *Optics Express*, vol. 12, no. 18, pp. 4261–4268, Sept. 2004.
- [17] Q. Xu, V. R. Almeida, and M. Lipson, “Time-resolved study of Raman gain in highly confined silicon-on-insulator waveguides,” *Optics Express*, vol. 12, pp. 4437–4442, 2004.
- [18] T. K. Liang and H. K. Tsang, “Pulsed-pumped silicon-on-insulator waveguide Raman amplifier,” *Proceedings of International Conference on Group IV Photonics*, 2004.
- [19] B. Jalali, V. Raghunathan, O. Boyraz, R. Claps, and D. Dimitropoulos, “Wavelength Conversion and Light Amplification in Silicon Waveguides,” *Proceedings of International Conference on Group IV Photonics*, 2004.
- [20] O. Boyraz and B. Jalali, “Demonstration of a silicon Raman laser,” *Optics Express*, Sept. 2004.
- [21] V. Raghunathan, D. Dimitropoulos, R. Claps, and B. Jalali, “Raman induced wavelength conversion in scaled Silicon waveguides,” *IEICE Electron. Express*, vol. 1, no. 11, pp. 298–304, Sept. 2004.
- [22] R. Claps, V. Raghunathan, D. Dimitropoulos, and B. Jalali, “Anti-Stokes Raman conversion in Silicon waveguides,” *Optics Express*, vol. 11, pp. 2862–2872, Nov. 2003.
- [23] J. J. Wynne, “Optical Third-Order Mixing in GaAs, Ge, Si, and InAs,” *Phys. Rev.*, vol. 178, pp. 1295–1303, 1969.
- [24] P. A. Temple and C. E. Hathaway, “Multiphoton Raman Spectrum of Silicon,” *Phys. Rev. B*, vol. 7, pp. 3685–3697, 1973.
- [25] M. Cardona and G. Guntherodt, *Light Scattering in Solids II*, Springer-Verlag, Berlin, 1982.
- [26] T. K. Liang and H. K. Tsang, “Role of free carriers from two-photon absorption in Raman amplification in silicon-on-insulator waveguides,” *Appl. Phys. Lett.*, vol. 84, no. 15, pp. 2745–2747, April 2004.

## 1 Introduction

Silicon has many desirable physical and economical properties that make it an attractive platform for optical and optoelectronic integration [1, 2]. The quality of commercial silicon wafers continues to improve while the wafer cost continues to decrease. At the same time, nanoscale device fabrication has entered volume manufacturing keeping alive the trend towards lower cost and higher performance. Silicon photonics may be considered as an extension of Silicon CMOS technology and that can provide high bandwidth interconnection between chips and within chips, and a platform technology for low cost optical components. Despite success in making high quality passive devices [2], silicon photonics has been hindered by the lack of active devices. Recently, good progress has been made in this direction. This includes light generation and amplification in Silicon Nanocrystals [3, 4], Er<sup>3+</sup> doped Silicon waveguide structures [5], and Er<sup>3+</sup> doped Silicon Nanocrystals [6, 7]. Optical modulation using MOS capacitance [8] and free carrier dispersion effects [9] and Photodetection using Silicon Germanium heterostructures [10].

Another approach towards realizing active functionalities in silicon is to make use of Raman scattering [11]. The Raman gain coefficient in silicon is nearly 10<sup>4</sup> times larger than that in glass fiber rendering this a plausible approach [11]. Silicon-on-insulator (SOI) platform is well suited for nonlinear optical devices because of the high index contrast between Silicon and silica ( $\Delta n \sim 2$ ), which results in strong optical confinement that tends to enhance nonlinear interactions. Exploiting these phenomena, spontaneous Raman emission from silicon waveguides was demonstrated in 2002 [11]. This was followed by demonstration of stimulated amplification [12] and coherent anti-Stokes Raman scattering [13], both in 2003. These observations followed earlier reports of Raman scattering in GaP waveguides [14]. Consequently, there has been increasing interest in Raman scattering in silicon with a number of reports this year describing net waveguide gain [15-17] and fiber-to-fiber gain [18, 19].

Recently, we have demonstrated the first silicon Raman laser [20]. In this paper, we report the first observation of Coherent Anti-stokes Raman Scattering (CARS) in a silicon Raman laser cavity. The laser is pumped by 1540 nm pulses and produces pulsed radiation at the Stokes wavelength of 1675. We show that the lasing at 1675 nm is accompanied with coherent anti-Stokes emission at 1427 nm, with identical threshold characteristics. After reaching the threshold pump level, both outputs grow linearly with increasing pump power level. To the best of our knowledge, this is the first ever observation of Coherent Anti-Stokes Raman Scattering (CARS) in any Raman laser, independent of the material system used.

## 2 Experimental results

### 2.1 The silicon Raman laser

Figure 1 shows the block diagram of the silicon Raman laser [20]. A mode locked fiber laser operating at 1540 nm with 25 MHz repetition rate is used

as a pulsed pump laser. After broadening the laser pulse width to 30 ps in a spool of standard Single Mode Fiber (SMF) and amplification, the pump pulses are coupled into the laser cavity by a Wavelength Division Multiplexer (WDM) coupler. The output of the WDM is coupled to the silicon waveguide which provides the optical gain. The waveguide is approximately 2 cm long with measured 0.8 dB fiber-to-fiber insertion loss. At the waveguide output, 95% of the power is looped back to the input WDM coupler to form laser ring cavity. Two Polarization Controllers (PC) are inserted on the pump arm and in the cavity to adjust the relative polarizations of the pump and the laser. The total length of the cavity is  $\sim 8$  m and adjusted to obtain 40 ns delay (the same as the pump period) at 1675 nm. The total cavity loss at 1675 nm is measured to be around 3.7 dB by using a CW signal at that wavelength. The 5% of the waveguide output is used to monitor the output. First, the laser output at 1675 nm is separated from the pump and the anti-Stokes. Then, another WDM coupler is used to extract the anti-Stokes wave. The temporal characteristics of the laser are measured by a 40 GHz oscilloscope and also with an autocorrelator. An Optical Spectrum Analyzer (OSA) is used to measure the spectrum.

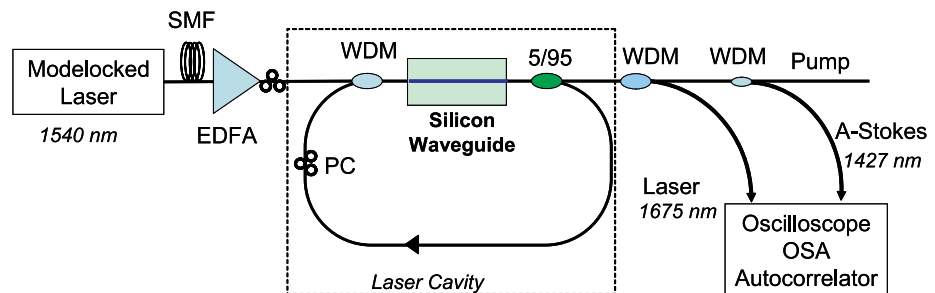


**Fig. 1.** Experimental set up used for silicon Raman laser demonstration. A ring cavity configuration is used as a resonator. A modelocked fiber laser at 1540 nm is used as a pump laser. The lasing is obtained at the Stokes wavelength of 1675 nm.

The measured laser output power variation with respect to average pump power is illustrated in Figure 2. The average pump power is varied from 0 to 15 mW to characterize the lasing behavior and to determine the lasing threshold. As shown in Figure 2, lasing, characterized by a sudden increase in emission at the Stokes wavelength of 1675 nm, is obtained when the average pump power level reaches to  $\sim 7$  mW, which correspond to the peak power level of 9 W. The threshold should occur when the waveguide gain compensates for the cavity loss and it is consistent with the measured cavity loss of 3.7 dB and the measured Raman gain of  $\sim 3.9$  dB at 9 W pump power. After exceeding the threshold level the output increases almost linearly with the pump power. It can readily be shown that lasing is caused by the Raman effect in silicon and not by the fibers, due to  $10^4$  times higher Raman gain coefficient in silicon [20]. At threshold, Raman gain in the 8 meter of fiber

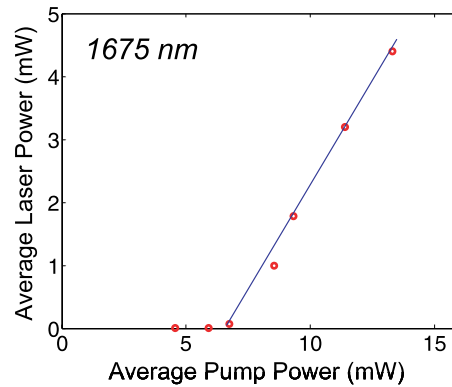


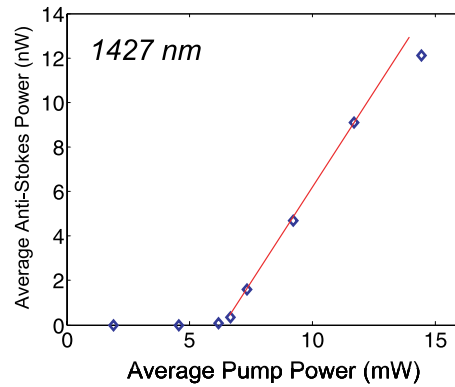
**Fig. 2.** Measured laser output power at 1675 nm. After reaching the threshold pump power of  $\sim 7$  mW the silicon starts lasing.

is  $< 0.2$  dB and is negligible compared to the measured open loop gain of 3.9 dB in silicon. Also, the spectral position of the laser output matches the Stokes wavelength of silicon but does not match the Raman gain peak in the fiber.

## 2.2 Coherent anti-Stokes emission

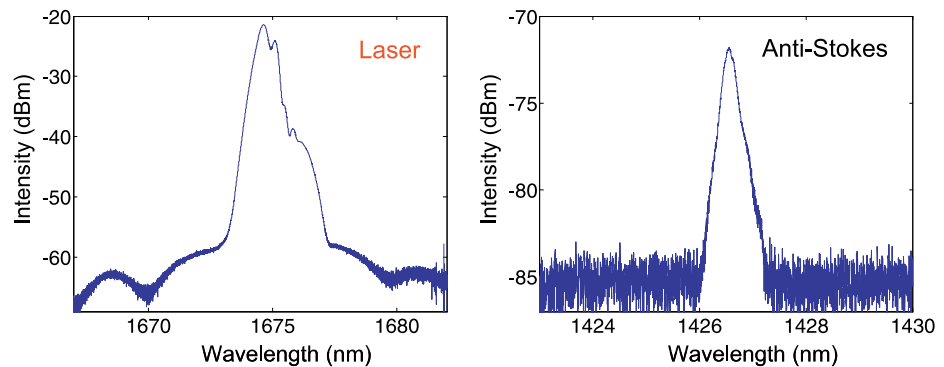
In stimulated Raman scattering, Stokes and anti-Stokes fields are simultaneously generated with the Stokes field experiencing amplification and exponential growth along the waveguide length. However, the extent to which the anti-Stokes is emitted depends on the phase mismatch between the pump ( $k_P$ ), Stokes ( $k_S$ ) and anti-Stokes ( $k_A$ ) fields, described by the relation:  $\Delta k = 2k_P - k_S - k_A$ . As  $\Delta k$  tends to be zero, the three fields experience strong parametric coupling leading to the exchange of information between the Stokes and anti-Stokes channels [21]. In this regime, the Raman nonlinearities can be used to perform wavelength conversion across widely spaced channels. This process has been used to demonstrate data conversion between the 1500 nm and 1300 nm bands [21, 22]. In Silicon this process is more efficient than four wave mixing based on the electronic susceptibility because the Raman susceptibility ( $\chi_R^{(3)} = 11.2 \times 10^{-14} \text{ cm}^2/\text{V}^2$ ) [22] is  $\sim 44$  times larger than the electronic counterpart ( $\chi_E^{(3)} = 0.25 \times 10^{-14} \text{ cm}^2/\text{V}^2$ ) [23]. However, the Raman process being resonant has a characteristic Lorentzian gain profile (bandwidth  $\sim 105$  GHz in Silicon) which determines the response of the conversion process to wavelength detuning from the peak.

Figure 3 illustrates the variation in the measure anti-Stokes power with respect to the average pump power. When the pump power reaches the lasing threshold level of 7 mW, anti-Stokes wavelength is observed. The cavity is designed for lasing at 1675 nm, and additionally, the circulation of anti-Stokes is blocked by the WDM coupler. Therefore, the system is not lasing at the anti-Stokes wavelength, but rather, the signal is due to parametric coupling between the lasing (Stokes) pump and anti-Stokes waves. This explains the much lower power levels at the anti-Stokes wavelength compared to the Stokes wavelength.



**Fig. 3.** Measured anti-Stokes power at 1427 nm. After reaching the threshold level, Raman coherent anti-Stokes signal is generated simultaneously with lasing.

Figure 4 presents the measured laser spectrum (4a) and that of the anti-Stokes signal (4b). The spectral peak of the silicon Raman laser is at the Stokes wavelength of 1675 nm, which is precisely the expected location based on the optical phonon frequency in silicon (15.6 THz) [11, 24, 25]. The 3 dB bandwidth of the laser is measured to be 0.36 nm ( $\sim 38.5$  GHz). The anti-Stokes laser, on the other hand, is centered at 1427 nm which is 15.6 THz up shifted from the pump wavelength. The frequency difference between the laser and the anti-Stokes is measured to be 31.2 THz, precisely twice the optical phonon frequency in silicon.



**Fig. 4.** Measured laser and pump spectra. The laser spectrum has 0.36 nm spectral bandwidth and is located 15.6 THz away from the pump laser. The pump-output separation is precisely the optical phonon frequency in silicon.

### 3 Summary

In this paper, we have reported the demonstration of a silicon Raman laser simultaneously producing coherent radiation at the Stokes and anti-Stokes wavelength. The signal at the Stokes wavelength is due to the lasing at that

wavelength whereas the anti-Stokes radiation is due to the parametric Raman coupling between the two signals and the pump. This suggests the possibility of silicon Raman laser with dual wavelength output. With a pump at around 1430 nm range, such a laser can simultaneously produce an output in both of the technologically important bands of 1300 nm and 1550 nm bands. Realization of this device requires a careful cavity design to accommodate both wavelengths. For better efficiency, waveguide should be engineered to obtain phase matching. In the present work, pulsed operation was necessary in order to avoid accumulation of free carriers that are generated due to TPA. Under CW operation, the free carrier losses would have reduced the net Raman gain and hence, would have prevented lasing. Carrier sweep out using a p-n junction can mitigate the free carrier losses and potentially yield CW operation [26].

### **Acknowledgments**

---

This work was supported by DARPA. The authors would like to thank Dr. Jagdeep Shah for his support. They also acknowledge Varun Raghunathan for technical discussions.